manuscripta geodaetica (1987) 12:86-98

manuscripta geodaetica

The Canadian geoid – Stokesian approach

Petr Vaníček and Alfred Kleusberg

Department of Surveying Engineering, University of New Brunswick, P.O. Box 4400, Fredericton, N.B., Canada E3B 5A3

Received August 19, 1986

ABSTRACT

The paper describes the theoretical aspects of the latest University of New Brunswick gravimetric solution of the Canadian geoid. Stokes's integral convolution approach reformulated for a higher-order reference field, GEM9 in this case, is used. In addition to the theoretical aspects, an example of the actual solution for eastern Canada is shown. Comparisons with Rapp's 1983 and Wenzel's GPM1 solutions, SEASAT altimetry and Canadian first-order Doppler points are also described.

1. INTRODUCTION

In this paper, we have restated the classical boundary value problem of geodesy and reformulated the solution. This reformulation led to the derivation of expressions for corrections to free-air gravity anomalies due to the presence of masses above the geoid, i.e., due to topography, and correction to the evaluated geoidal height due to the formulation of the boundary value problem, i.e., the indirect effect. These are not new, but we could not find them in the literature and decided to include them here for the sake of completeness.

To make use of the integrity of the long wavelength part of the geoid determined from satellite orbit perturbations, we use the GEM9 solution for a higher-order reference spheroid. (We use the word ***spheroid*** in its literary meaning—a sphere-like body—rather than to describe a bi-axial ellipsoid.) For easy comparisons, we relate this reference spheroid to the GRS80. The use of a higher-order reference spheroid and reference gravity field results in the necessity to reformulate the integration kernel in the Stokes convolution. This new kernel we call the ***spheroidal kernel***. It differs from the standard Stokes kernel by the fact that it lacks the low frequency part and tapers off more rapidly. Thus the integration does not have to be carried out too far.

The numerical integration is done in a more or less standard way. We use a 10 by 10 minute rectangular innermost zone in which the integration is done semi-analytically, using point gravity anomalies. In the inner zone, whose outside boundary is also rectangular (2 by 2 degrees), we use a purely numerical approach employing 5 by 5 minute mean gravity anomalies. In the outer zone, bounded outside by a radius of 6°, 1 by 1 degree mean gravity anomalies are used. To minimize the error of integration truncated at 6° radius, the spheroidal kernel was modified using Molodenskij's truncation coefficients. In the inner and outer zone integration, the modified spheroidal kernel is approximated by a linear form to further speed up the computations. We have determined experimentally that the discretization error of this numerical integration is not more than 10 cm.

We have produced several iterations of this gravimetric geoid for the area of $42° \leq \phi \leq 70°$ and $219°E \leq \lambda \leq 317°E$, i.e., about 2×10^7 km^2, on a 10 by 10 minute geographical grid. The first solution was produced for the Geodetic Survey of Canada at the beginning of 1986 under a research contract. Comparisons of our latest, December 1986, geoid with Rapp's 1983 (180, 180) and Wenzel's 1985 GPM 1 truncated to (180, 180) solutions show an r.m.s. error of about 1 metre. Comparison with 212 Doppler points in Canada shows a positive bias of 79 cm and an r.m.s. error of 1.7 m. The fit to SEASAT altimetry in Hudson Bay and in the eastern Canadian offshore is significantly

---

Offprint requests to: P. Vaníček

better, with a negative bias of 19 cm and an r.m.s. error of 53 cm.

Work is now going forward on an implementation of a scheme for the incorporation of other kinds of data for further improvement of the geoid.

2. FORMULATION OF GEODETIC BOUNDARY VALUE PROBLEM

The classical formulation of the geodetic boundary value problem reads as follows: Let the disturbing potential T be defined by

$$T = W - U\,, \tag{1}$$

where W is the actual gravity potential, and U is an appropriately chosen reference potential. If the centrifugal parts of W and U are identical, then the Laplace equation

$$\nabla^2 T = 0 \tag{2}$$

is valid outside the gravitating masses of the earth. To satisfy the Laplace equation, we shall assume, for the time being, that all these masses are trapped inside the geoid; the consequences of this condition not being rigorously satisfied will be discussed below.

Let us assume further that U has been chosen so that it has a constant value U_o, equal to the actual gravity potential value W_o on the geoid, on a geocentric reference ellipsoid. Then the height N of the geoid above the reference ellipsoid is given by Bruns's formula:

$$N = T_G/\gamma_o\,, \tag{3}$$

where the subscript G refers to the geoid, while γ_o is the normal gravity on the reference ellipsoid [Heiskanen and Moritz, 1967].

Next, we take a derivative of eqn. (1) with respect to the outer normal n of the reference ellipsoid and evaluate it on the geoid to get

$$\partial T/\partial n|_G = \partial W/\partial n|_G - \partial U/\partial n|_G\,. \tag{4}$$

Here, $\partial U/\partial n|_G$ equals $-\gamma_G$ exactly, while $\partial W/\partial n|_G \doteq -g_G$ to a sufficient degree of accuracy (better than 10 μGal). Adding and subtracting γ_o we have

$$\partial T/\partial n|_G = - g_G + \gamma_o + \gamma_G - \gamma_o\,, \tag{5}$$

which can be rewritten, using the same degree of approximation as for the derivative above, as

$$\Delta g = - \partial T/\partial H|_G + \partial\gamma/\partial n|_G\, N\,, \tag{6}$$

where the height H is reckoned along the actual plumbline. The vertical gradient of normal gravity in 'spherical' approximation (good to the order of flattening) equals $2\gamma_o/R$ and realizing that, according to Bruns's formula, $N\gamma_o$ equals T_G, we get finally

$$\Delta g = - \partial T/\partial H|_G - (2/R)T|_G\,. \tag{7}$$

Equation (7) shows that Δg can serve as boundary values of mixed type for the solution of the Laplace eqn. (2). We note that the boundary values pertain to the **geoid** and not, as incorrectly stated by Vaníček and Krakiwsky [1982, p.516], to the reference ellipsoid. Even though the gravity anomaly refers to either of the two surfaces (ellipsoid or geoid), the right-hand side of eqn. (7) refers to the geoid only.

The solution T to the geodetic boundary value problem is usually sought in terms of Stokes's integral [Heiskanen and Moritz, 1967]. This integral can then be converted into Stokes's formula for geoidal heights,

$$N(\phi, \lambda) = R/(4\pi\gamma) \oint\!\!\oint_E \Delta g(\phi', \lambda')\, S(\psi)\, dv\,, \tag{8}$$

where dv is an element of a spatial angle. It should be noted that Stokes's formula is blind to the selection of U_o, and thus Δg_o, i.e., the mean global value of gravity anomaly. The computed value N always corresponds to $\Delta g_o = 0$ and is thus referred to as the "best fitting" geocentric reference ellipsoid, whatever its size is. The Stokes function S, a function of spherical distance ψ between (ϕ, λ) and (ϕ', λ'), has a series expansion

$$S(\psi) = \sum_{k=2}^{\infty} (2k+1)/(k-1)\, P_k(\cos\psi) \tag{9}$$

with P_k being Legendre polynomials of degree k [Abramowitz and Stegun, 1964].

3. CORRECTIONS

The above solution assumes the disturbing potential T to be harmonic outside the geoid, i.e., the masses outside the geoid to be absent. This condition is violated by both the atmosphere and the topographical masses of the earth. The effects of both now have to be removed.

The atmospheric masses attract any element on the surface of the earth, thus changing the gravity reading to $g + \delta g_A$. This **atmospheric attraction effect** was investigated by Ecker and Mittermayer [1969] and tables for δg_A have been published by IAG [1971]. The effect is a function of height and varies between -0.87 mGal and -0.54 mGal for heights ranging from 0 to 4 km. The second-order effect caused by the irregularity of the lower boundary of the atmosphere [Vaníček and Krakiwsky, 1982, p.166] is not considered here.

Using free-air gravity anomaly in eqn. (8) is equivalent to the 'squashing' of all the topographical masses onto the geoid. So dislocated masses satisfy the basic assumption of the boundary value problem. But they also change the gravitational attraction on the earth's surface: this trick introduces a **topographical attraction** effect δg_T which has to be added to the free-air anomaly Δg before this is used in the Stokes formula.

To evaluate this topographical effect, it is adequate to approximate the geoid by a horizontal plane and assign a constant density σ to all the topographical masses (cf. Figure 1). For integration areas up to 6° and topographic height differences up to 2 km, the planar approximation leads to errors less than $1 \cdot 10^{-3}$. A mass element dm located at a height $H_A + z$, below point P_Q,

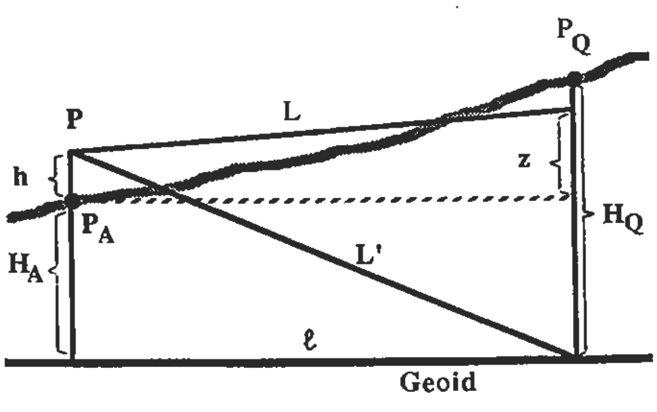

FIGURE 1
Computation of the topographical attraction effect.

causes at point P an increase of gravity potential by $dW = dm/L$. The same element placed onto the geoid causes at P an increase by $dW' = dm/L'$. Hence, when dm is 'squashed' onto the geoid (from its original position $H_A + z$ above the geoid), the observer at P_A will experience a change in gravity equal to

$$\delta g_T = \partial/\partial h \, (dW - dW')|_{h=0} \,. \qquad (10)$$

The total change in g at point P_A is obtained through integration over all the mass elements dm contained in the topography. We get

$$W = G\sigma \int_{\alpha=0}^{2\pi} \int_{l=0}^{\infty} \int_{z=-H_A}^{H_Q-H_A} l/L \, dz \, dl \, d\alpha \qquad (11)$$

$$W' = G\sigma \int_{\alpha=0}^{2\pi} \int_{l=0}^{\infty} l/L' \, H_Q \, dl \, d\alpha \,. \qquad (12)$$

It can be shown that the infinite plate of constant thickness H_A and density σ causes at P_A a gravitational attraction identical to that caused by the same masses concentrated at the lower surface of this plate (i.e., on the geoid). These two effects thus can be subtracted in eqns. (11) and (12) giving for the topographical effect (cf. eqn. (10)):

$$\delta g_T = G\sigma \, \partial/\partial h \{ \int_{\alpha=0}^{2\pi} \int_{l=0}^{\infty} [\int_{z=0}^{H_Q-H_A} L^{-1} \, dz - \qquad (13)$$

$$- (H_Q - H_A) L'^{-1}] \, l \, dl \, d\alpha |_{h=0} \,.$$

Expressing L^{-1} and L'^{-1} in a power series of H_A/l, h/l, and z/l to an accuracy of second-order terms and performing the differentiation of the subintegral function with respect to h, we obtain:

$$\delta g_T \doteq 1/2 G\sigma \int_{\alpha=0}^{2\pi} \int_{l=0}^{\infty} (H_Q^2 - H_A^2) l^{-3} \, dA \,, \qquad (14)$$

where $dA = l \, dl \, d\alpha$. We note that because of the rapid decrease of the kernel l^{-3} in the above integral, the integration has to be performed only in the immediate neighbourhood of the point of interest.

The (mathematically conducted) 'squashing' of the topographical masses onto the geoid — and the subsequent correction of observed free-air anomalies — has the unfortunate consequence that the computed geoid is distorted. This is the **indirect effect** [Heiskanen and Moritz, 1967] that can be computed as

$$\delta N_I = \delta W_I/\gamma , \tag{15}$$

where δW_I is the difference of gravitational potentials of the actual topographical masses and squashed masses. This difference must be reckoned on the geoid and can be evaluated in planar approximation from equations similar to eqns. (11) and (12) as (cf. Figure 2):

$$W_I = G\sigma \int_{\alpha=0}^{2\pi} \int_{l=0}^{\infty} \int_{z=0}^{H_Q} l/L \, dl \, d\alpha \, dz$$

$$W'_I = G\sigma \int_{\alpha=0}^{2\pi} \int_{l=0}^{\infty} H_Q \, dl \, d\alpha \ . \tag{16}$$

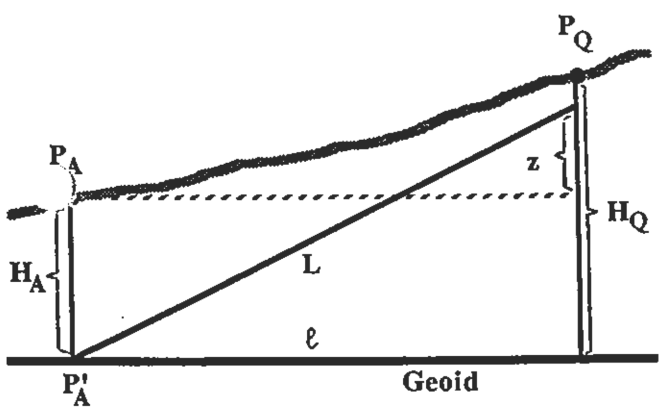

FIGURE 2
Computation of the indirect effect.

It is expedient to evaluate the indirect effect potential $\delta W_I = W_I - W'_I$ separately for the plate, P, of uniform thickness H_A and for the excess of the topography with respect to this plate. Equations (16) yield:

$$\delta W_{IP} = G\sigma \int_{\alpha=0}^{2\pi} \int_{l=0}^{\infty} [\int_{z=0}^{H_A} l(l^2 + z^2)^{-1/2} \, dz - H_A] \, dl \, d\alpha$$

$$\delta W_{IT} = G\sigma \int_{\alpha=0}^{2\pi} \int_{l=0}^{\infty} [\int_{z=H_A}^{H_Q} l(l^2+z^2)^{-1/2} \, dz - H_Q + H_A] \, dl \, d\alpha \ . \tag{17}$$

The first integral is solved by integrating first with respect to α and l getting

$$\delta W_{IP} = 2\pi G\sigma \lim_{l \to \infty} \{ \int_{z=0}^{H_A} [\sqrt{(l^2 + z^2)} - z] \, dz - l \, H_A \} \ .$$

Integration with respect to z, expansion of the square root and logarithmic functions into power series and performance of the limiting operation gives

$$\delta W_{IP} \doteq - \pi G\sigma H_A^2 \ . \tag{18}$$

The second integral is solved by first integrating with respect to z and then expanding the square root and logarithmic functions into power series. We then get

$$\delta W_{IT} \doteq - G\sigma/6 \int_{\alpha=0}^{2\pi} \int_{l=0}^{\infty} (H_Q^3 - H_A^3) l^{-3} \, dA \ . \tag{19}$$

Combining eqns. (18) and (19) we finally obtain:

$$\delta N_I \doteq - (\pi G\sigma)\gamma^{-1} H_A^2 - \\ - G\sigma\gamma^{-1}/6 \int_{\alpha=0}^{2\pi} \int_{l=0}^{\infty} (H_Q^3 - H_A^3) l^{-3} \, dA \ . \tag{20}$$

Here, once more, the rapid decrease of l^{-3} guarantees a rapid convergence of the integration which, consequently, can be done only over the immediate neighbourhood of the point of interest.

4. REFORMULATION OF STOKES'S SOLUTION FOR A HIGHER-ORDER REFERENCE FIELD.

Stokes's solution, in its original form, of the geodetic boundary value problem presupposes a geocentric ellipsoid for the reference surface. The integration (8) has to be carried out theoretically to a distance $\psi = 180°$ and practically to a distance of many tens of degrees from the point of interest, i.e., to a distance of many thousands of kilometres. Yet the coverage with terrestrial data is quite inhomogeneous — while at places it is almost adequate on land, it leaves a lot to be desired at sea. This problem is alleviated if a higher-order reference surface is used: the Stokes function that refers to a higher-order surface (higher-order spheroid) drops down to zero more rapidly than the ordinary (second order) Stokes function (eqn. (9)) and the integration does not have to be carried out that far (see, e.g., Vaníček and Krakiwsky [1982]). We call such Stokes's function a **spheroidal Stokes's function**. If the reference spheroid is given by spherical harmonic functions up to degree and order l, then the spheroidal Stokes function that should be used on this spheroid is (see, Vaníček and Krakiwsky [1982, p.574])

$$S_{l+1} = \sum_{k=l+1}^{\infty} (2k+1)/(k-1)\, P_k(\cos\psi)\,. \qquad (21)$$

The graph of such spheroidal Stokes's function for l=20 is shown in Figure 3.

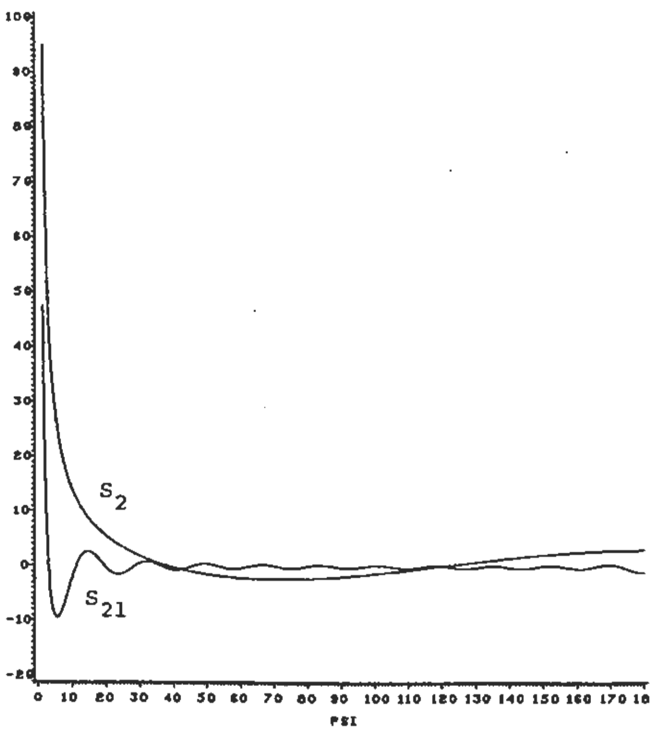

FIGURE 3
Graph of the spheroidal Stokes function S_{21}.

The additional advantage of using the higher-order reference field is that the detrimental effect of the spherical approximation used in the derivation of Stokes's formula (see above) is significantly attenuated. This is because the effect is mostly of long wavelengths [Rapp, 1981] which disappear when the spheroidal Stokes function is used.

The low degree gravitational field, and thus the long wavelength part of the geoid, is quite well determined through the analysis of satellite orbits. It is, therefore, natural to take a satellite determined low-order field to define a reference spheroid which would then be used to refer the higher-order (more detailed) geoidal features to. This is the approach we have chosen to follow here, having had good experience with it before [Vaníček and John, 1983].

5. SELECTION OF THE REFERENCE SPHEROID

Out of the variety of available satellite derived potential fields, we have chosen to adopt the GEM9 [Lerch et al., 1979], the time proven pure satellite solution. GEM9 is complete to degree and order 20, and no improvement to this solution from terrestrial data has been attempted here. This means that only features smaller (in spatial extent) than 9° (or 1000 km) will have to be picked up by the terrestrial gravity contribution.

Further, to be able later to compare our results to those of other people, we have decided to refer the GEM9 solution to the Geodetic Reference System 1980 (GRS80). The GRS80 normal potential is given by [Moritz, 1980]:

$$U_{GRS80}(r, \phi, \lambda) = GM^* r^{-1} \Big[1 - \sum_{n=2,4,6,8} (a^*/r)^n J_{n0}^* Y_{n0}^c(\phi, \lambda)\Big]\,, \qquad (22)$$

where the asterisk is used to distinguish the GRS80 values from corresponding GEM9 values. The GEM9 defined disturbing potential T' referred to GRS80 is then

$$T'(r, \phi, \lambda) = (GM - GM^*) r^{-1} + $$
$$+ GMa^{-1} \sum_{n=2}^{20} \sum_{m=0}^{n} (a/r)^{n+1} (\Delta J_{nm} Y_{nm}^c + \Delta K_{nm} Y_{nm}^s), \qquad (23)$$

where (GM-GM*)/r represents a scale change, $T_0(r) = U_0(r)$, in the reference (normal) potential between GRS80 and GEM9, while ΔJ, ΔK are the differences between the actual (GEM9) and normal (GRS80) potential coefficients.

In eqn. (23), all ΔK— are clearly equal to zero and so are the ΔJ— for $n \neq 2,4,6,8$, or $m \neq 0$. For n=2,4,6,8 we find

$$\Delta J_{no} = J_{no} - GM^*/(GM)\,(a^*/a)^n\,\tilde{J}^*_{no}\,, \tag{24}$$

where $\tilde{J}^*_{no}$ are normalized GRS80 coefficients (through division by $\sqrt{(2n+1)}$) to conform with the expression s for J_{no} used in the definition of the GEM9 system. Multiplication by

$$GM^*/GM\,(a^*/a)^n \doteq 1 - (0.351 + 0.470\,n) \times 10^{-6} \tag{25}$$

of the normalized GRS80 coefficients [Moritz, 1980] yields

$$\begin{aligned} J'_{20} &= 484.166\,86 \times 10^{-6}, \\ J'_{40} &= -0.790\,30 \times 10^{-6}, \\ J'_{60} &= 0.001\,69 \times 10^{-6}, \\ J'_{80} &= -3.5 \times 10^{-12}\,. \end{aligned} \tag{26}$$

Equation (24) then gives

$$\begin{aligned} \Delta J_{20} &= 0.000\,68 \times 10^{-6}, \\ \Delta J_{40} &= -0.248\,76 \times 10^{-6}, \\ \Delta J_{60} &= -0.149\,52 \times 10^{-6}, \\ \Delta J_{80} &= J_{80}\,. \end{aligned} \tag{27}$$

Finally, eqn. (23) divided by γ gives the height N_{GEM9} of the GEM9-defined reference spheroid above the GRS80 reference ellipsoid. We note that when, at the end, the geoidal height is sought above the GRS80 reference ellipsoid, N_{GEM9} has to be added to the δN obtained from terrestrial gravity anomalies through (integral) convolution with the spheroidal Stokes function S_{21} (cf. §4).

The error in the GEM9 reference spheroid with respect to the GRS80 reference ellipsoid can be obtained from the GEM9 degree variances σ_n^2 [Lerch et al., 1984]. Assuming the potential coefficients to be uncorrelated, we get for the average standard deviation in N_{GEM9}:

$$\delta N_{GEM9} = R \sqrt{\sum_{n=2}^{20} (2n+1)\,\sigma_n^2}\,. \tag{28}$$

The average standard deviation reaches the value of about 1.75 m for degree 20. It must be noted, however, that this is a purely long wavelength error ($\geq$ 1000 km).

6. NUMERICAL INTEGRATION

The integration of terrestrial gravity anomalies with the spheroidal Stokes function has to be done numerically. For the sake of computational economy, it is, of course, desirable to limit the size of the integration area as much as possible without compromising the accuracy to an unacceptable degree. It is, as stated above, much easier to do this with the spheroidal than the ellipsoidal Stokes functions.

We have decided to use a spherical cap with as small a radius ψ_o as possible. Not to degrade the accuracy unnecessarily through the truncation of the radius of the integration area from π to ψ_o, we modify the spheroidal Stokes function following the idea of **truncation coefficients** [Molodenskij et al., 1960]. We get for the modified spheroidal Stokes function $S_l^m(\psi)$ the following expression:

$$S_{l+1}^m(\psi) = S_{l+1}(\psi) - \sum_{i=0}^{l} 1/2(2i+1)\, t_i\, P_i(\cos\psi)\,, \tag{29}$$

where the t_i coefficients are determined from the system of linear equations:

$$\sum_{k=0}^{l} (2k+1)\, e_{ik}(\psi_o)\, t_k = 2Q_i^l(\psi_o) \qquad \forall i\,. \tag{30}$$

Here

$$e_{ik}(\psi_o) = \int_{\psi=\psi_o}^{\pi} P_i(\cos\psi)\, P_k(\cos\psi)\, \sin\psi\, d\psi\,, \tag{31}$$

and

$$Q_i^l(\psi_o) = Q_i(\psi_o) - \sum_{j=2}^{l} (2j+1)/(j-1)\, e_{ij}(\psi_o)\,, \tag{32}$$

where

$$Q_i(\psi_o) = \int_{\psi=\psi_o}^{\pi} S(\psi)\, P_i(\cos\psi)\, \sin\psi\, d\psi \tag{33}$$

are the Molodenskij truncation coefficients. Paul's [1973] recursive algorithm is used to compute these truncation coefficients. The spheroidal kernel S_{21} and its modified form $S_{21}{}^m$ for ψ_o=6° are shown in Figure 4. It should be pointed out that other approaches to kernel modification exist (see, e.g., Jekeli [1981] or Sjöberg [1986]). We are, at present, looking into possible improvements to our solution using a different modification.

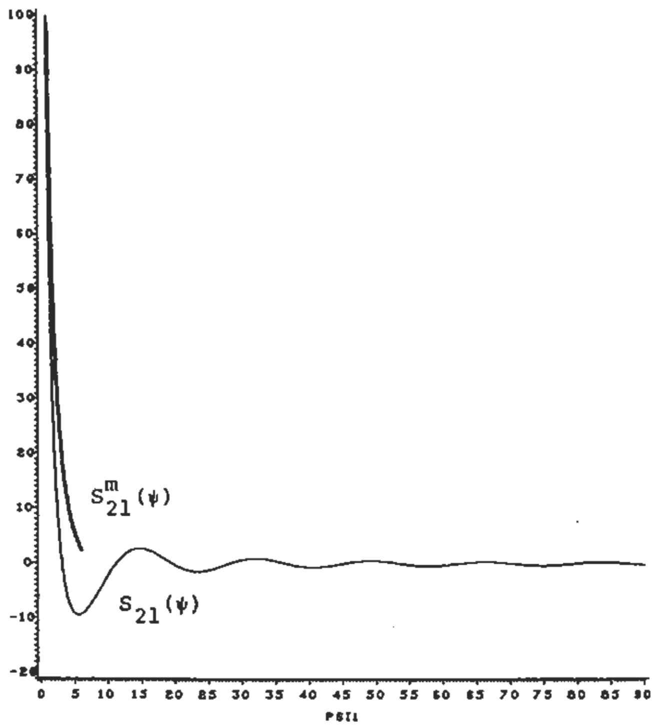

FIGURE 4
Spherical Stokes's kernel S_{21} and its modified form $S_{21}{}^m$.

The following point must be noted: Because of orthogonalities, it does not matter in the convolution of Δg with the original S_l, if Δg has had the low degree constituents (corresponding to the reference spheroid) subtracted from it or not (cf. Vaníček and Krakiwsky [1982, p.574]). It does matter, however, when integration with the modified kernel $S_l{}^m$ is used: the low degree constituents must be subtracted from Δg beforehand because the modified kernel is no longer 'blind' to low frequencies. For the GEM9 reference spheroid and GRS80 normal gravity, we have

$$\Delta g' = \Delta g - \Delta g_{GEM9}\,, \qquad (34)$$

where Δg_{GEM9} is obtained from T'_{GEM9} (eqn. (23) using eqn. (7):

$$\Delta g_{GEM9} = -\,\partial T'_{GEM9}/\partial r - 2R^{-1}\,T'_{GEM9}\,. \qquad (35)$$

A 1° × 1° mesh in ϕ, λ coordinates is the basi graticule for the numerical integration. The integratio cap is approximated by the area covered with 1° × 1 ellipsoidal rectangles whose centres are no further awa from the point of interest than ψ_o degrees. Thi approximated area is then divided into three zones:

(1) The **innermost zone**, which covers the immediat 10' × 10' neighbourhood of the point of interest (1(× 20' for high latitudes). Its boundaries coincid with the grid lines of the 5' × 5' gravity anomaly fil (see section 7) and the point of interest thus may no be in the exact centre of the innermost zone.
(2) The **inner zone** covers an area of 2° × 2° (minu the innermost zone). Its outer boundaries coincid with the grid lines of the 1° × 1° gravity anomal file (see section 7).
(3) The **outer zone** covers the area between the oute boundary of the inner zone and the boundary of th whole integration area.

Subdivision into the three zones was introduced t allow for the use of different mean gravity anomaly dat sets and different, as efficient as possible, integratio techniques. The exact location of the two innne (rectangular) boundaries does not seem to matter ver much: even significant shifts of these boundaries caus changes of resulting δN of the order of at most a fe centimetres. On the other hand, location of the outsid boundary, i.e., of ψ_o, matters a great deal. After som experimentation (see Vaníček et al. [1986a]) we hav settled on ψ_o=6°. This selection ensures that th discretization error (error due to the numerica evaluation of Stokes's formula) is below 10 centimetres.

The integration in the innermost zone is done in a semi-analytical way. First, a second-order algebraic surface (with 6 mixed algebraic terms) is fitted in the least-squares sense to all the available point gravity anomalies available in the innermost zone. If there are not enough data, the number of terms is lowered by 2 then by another 1 at which instance the four 5' × 5' mean anomalies falling into the innermost zone are taken instead of point anomalies. The decision as to whether to lower the order of the surface is based on the value of the ratio of the smallest and largest eigenvalues of the normal equations for the surface coefficients. In the north, where the 5' × 5' mean anomalies are replaced by 5' × 10' mean anomalies (see below), the selection is modified so that the default value is the average of the two mean anomalies.

To an accuracy of at least 0.01%, the modified spheroidal Stokes function $S_{l+1}{}^m$ in the innermost zone can be replaced by [Vaníček et al., 1986a]:

$$S_{l+1}{}^m(\psi, \psi_o) = 2/\psi - 3\ ln\ \psi/2 + C(\psi_o)\ , \qquad (36)$$

where $2/\psi$ is the dominant term,

$$C(\psi_o) = -4 - \sum_{i=2}^{l} (2i+1)/(i-1) - \sum_{i=0}^{l} 1/2(2i+1)\ t_i(\psi_o)\ , \qquad (37)$$

and the t_i-coefficients are given by eqn. (30). The product of the two series (one for $S_{l+1}{}^m$ and one for Δg), now containing 24 terms, can be ordered then in descending order of significance. We retain only the 8 most significant terms and integrate these term by term. Finally, re-arrangement of these 8 terms yields, for the innermost zone contribution:

$$\delta N_{INM} = \sum_{j=0}^{5} \hat{\alpha}_j\ I_j(\psi_o)\ , \qquad (38)$$

where $\hat{\alpha}_j$ are the least-squares estimates of the anomaly surface coefficients, and $I_j(\psi_o)$ are numbers determined through the integration. For details, we refer the reader to Vaníček et al. [1986a].

In the numerical integration over the inner and outer zones, the integral is simply replaced by the following summation:

$$I = R/(4\pi\gamma) \sum_{j=1}^{J} S_{l+2}{}^m(\psi_j, \psi_o)\ \overline{\Delta g}'_j\ A_j\ , \qquad (39)$$

where $\overline{\Delta g}'_j$ is the mean gravity anomaly for the j^{th} cell (5' × 5' or 1° × 1°), A_j is the area of the cell

$$A_j = a \cos\phi_i\ , \qquad (40)$$

with a being the size of the cell (5' or 1°) in radians, and ϕ_i refer to the centre point of the cell.

The evaluation of $S_{l+1}{}^m(\psi_j, 6°)$ for each cell is a time consuming task. It has to be done 572 times for the inner zone and at least 164 times for the outer zone (for $\phi >$ 45°), or half as many times if advantage is taken of longitudinal symmetry. We have hence decided to approximate the modified spheroidal Stokes function by the following linear form:

$$\tilde{S}_{l+1}{}^m(\psi, \psi_o) = \beta_o + \beta_1/\psi + \beta_2\ ln\ (\psi/2) + \beta_3\ \psi^2\ ln\ (\psi/2)\ . \qquad (41)$$

Here, the coefficients are functions of ψ_o and are selected in such a way as to make $\tilde{S}$ fit the modified kernel $S_{l+1}{}^m$ as well as possible in the uniform (Tchebyshev) sense.

The selection has been done approximately — being unaware of the existence of any rigorous algorithm — by moving the four needed Tchebyshev interpolation nodes until a good fit has been achieved. The resulting values:

β_o = - 32.435,
β_1 = 2.0,
β_2 = -3.449,
β_3 = - 173.24,

give for the six-degree radius of integration the maximum relative errors in $\tilde{S}$ less than 10^{-3}. Tests conducted on several sets of gravity anomalies showed that errors in the geoid committed by using this approximation are within 1 centimetre. Clearly, alternative techniques exist. Their relative merits should be investigated.

Integration for both the topographical effect (eqn. (14)) and indirect effect (eqn. (20)) also have to be done numerically. The topographical effect integral is rewritten as

$$\delta g_T = 1/2G\sigma R^2 \sum_i (H_i^2 - H_A^2) l_i^{-3} A_i\ , \qquad (42)$$

where H_i, l_i, A_i refer to the i^{th} 5' × 5' cell and the summation extends over all cells with significant contributions. Similarly, the indirect effect is evaluated from:

$$\delta N_I = \pi G\sigma\gamma^{-1} H_A^2 - G\sigma R^2\gamma^{-1}/6 \sum_i (H_i^2 - H_A^2) l_i^{-3} A_i\ , \qquad (43)$$

where, once more, 5' × 5' cells are used.

7. GRAVITY DATA

The point gravity data used in this study come from two files supplied by the Division of Gravity, Geothermics and Geodynamics of the former Earth Physics Branch of Energy, Mines and Resources Canada [Hearty, 1985; 1986]. The union of the two files contains 628 019 records, each consisting of ϕ, λ, $\Delta g'$ (free-air anomaly minus GEM9 modelled value), $\sigma_{\Delta g}$, H, σ_H. The observed values of g are referred to IGSN71, γ refer to GRS80, and the points fall into an area delimited by parallels 40°N and 80°N and meridians 218°E and 320°E. Both land and sea values are included.

The 5' × 5' mean gravity anomalies come from the same source [Winter, 1979]. The file, however, has been updated by us by predicting additional means for about 3000 originally empty cells. These have been determined as ordinary arithmetic means of values contained in the point anomaly file. For each cell we have: $\overline{\Delta g}'$ (the mean free-air anomaly corrected for GEM9), $\sigma_{\overline{\Delta g}}$, and H.

The 5' × 5' cells cover only the latitudinal belt between 40°N and 56°N (214°E ≤ λ ≤ 318°E). From 56°N to 76°N the size of the cells is extended to 5' × 10' to maintain at least a resemblance of equi-areality. Empty cells exist reflecting the lack of point gravity values in certain areas. These empty cells, in turn, are treated in such a way that if any one of them happens to fall within the inner zone of Stokes's integration, i.e., within a 2° × 2° rectangle containing the point of evaluation, the value of the corresponding 1° × 1° gravity anomaly is used in the integration with a standard deviation of 50 mGal.

Finally, the 1° × 1° mean anomalies were obtained from the Department of Geodetic Science and Surveying of Ohio State University (OSU). These data are termed "The January 1983 1 × 1 Degree Mean Free-air Anomaly Data" [Rapp, 1983a]. In our area of interest (30°N ≤ ϕ ≤ 80°N), (190°E ≤ λ ≤ 340°E) there have been 185 cells containing no other information except for the height. For 24 of these, we were able to compute the mean anomaly, again using the point gravity file. The standard deviation is determined as half of the absolute value of the computed mean anomaly corrected for the GEM9 contribution. The remaining empty cells are used in the integration with $\overline{\Delta g}'$ equal to zero and $\sigma_{\overline{\Delta g}}$ equal to 50 mGal.

8. RESULTS

We have produced the geoid, i.e., the sum of GEM9 and the terrestrial gravity contribution, all referred to the GRS80 on a 10 by 10 minute grid covering an area of: 42°N ≤ ϕ ≤ 70°N, 219°E ≤ λ ≤ 317°E. An example of this solution for eastern Canada and part of the United States is shown in Figure 5. Plotted at a larger scale, the geoid looks, of course, much the same as other solutions and we do not show it here. The estimated standard deviation for the gravimetric part (medium and short wavelength) ranges between 7 and 35 cm.

Comparisons with other, 'independent' solutions and values yield the following:

(a) Rapp 1983 (180, 180) solution [Rapp, 1983b] — for differences evaluated on a 1° × 1° grid, the mean difference N_{Rapp} - N_{UNB} equals +94 cm with an r.m.s. (with respect to that mean) of 106 cm. The plot of these differences is shown in Figure 6. Regarding this comparison, Rapp's solution is referred to an ellipsoid with major semi-axis probably one metre smaller than the GRS80 ellipsoid [Rapp, 1983b], which would explain the 94 cm bias seen here. Also, a substitution of the GEML2 model [Lerch et al., 1982] for GEM9 would result in a significant reduction of the r.m.s. quoted here [Rapp, 1986]. This aspect is now being investigated.

(b) Wenzel GPM1 solution [Wenzel, 1985] truncated for computational reasons to (180, 180) — for differences evaluated on a 1° × 1° grid, the mean difference N_{Wen} - N_{UNB} is +55 cm with an r.m.s. of 95 cm. These differences are plotted in Figure 7.

(c) Heights of 212 Doppler points in Canada [Geodetic Survey of Canada, 1985] above the GRS80 minus their orthometric heights — the mean difference is +79 cm with an r.m.s. of 170 cm.

(d) OSU adjusted SEASAT altimetry [Rapp, 1982] gridded at UNB [Vaníček et al., 1986b] in Hudson Bay and the eastern Canadian offshore (for ϕ ≤ 68°) — for differences evaluated on 10 × 10 minute grid, the mean difference is -19 cm with an r.m.s. error of 65 cm. The differences, which can be interpreted as the computed sea surface topography, are shown in Figure 8.

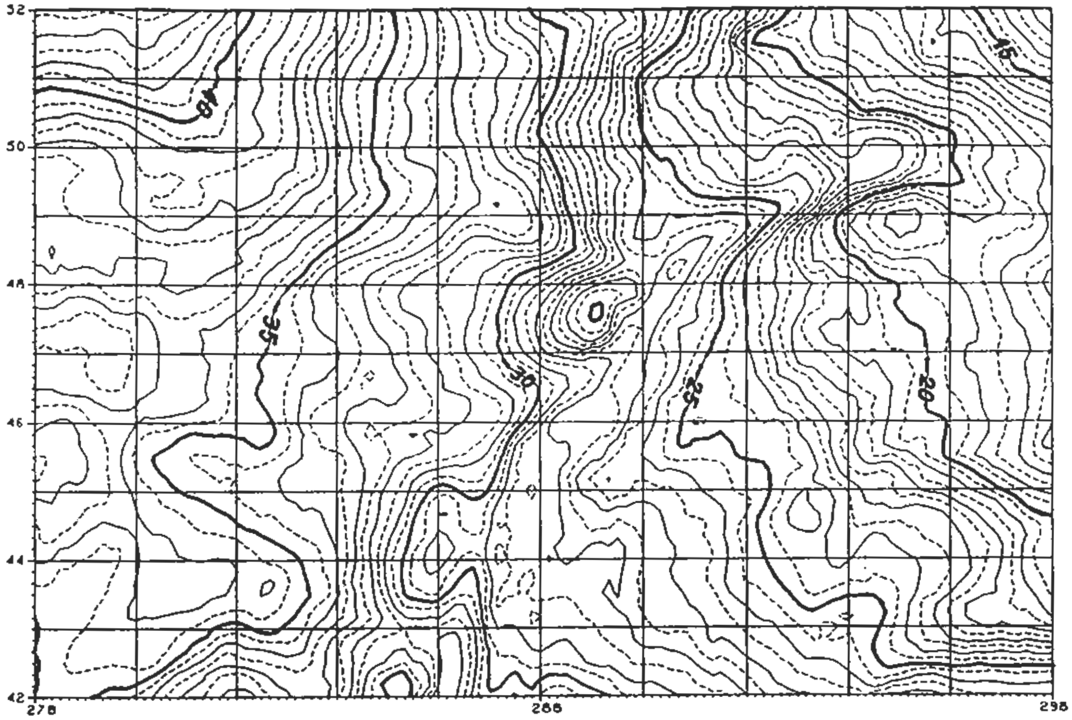

FIGURE 5
Part of the gravimetric Canadian Geoid.

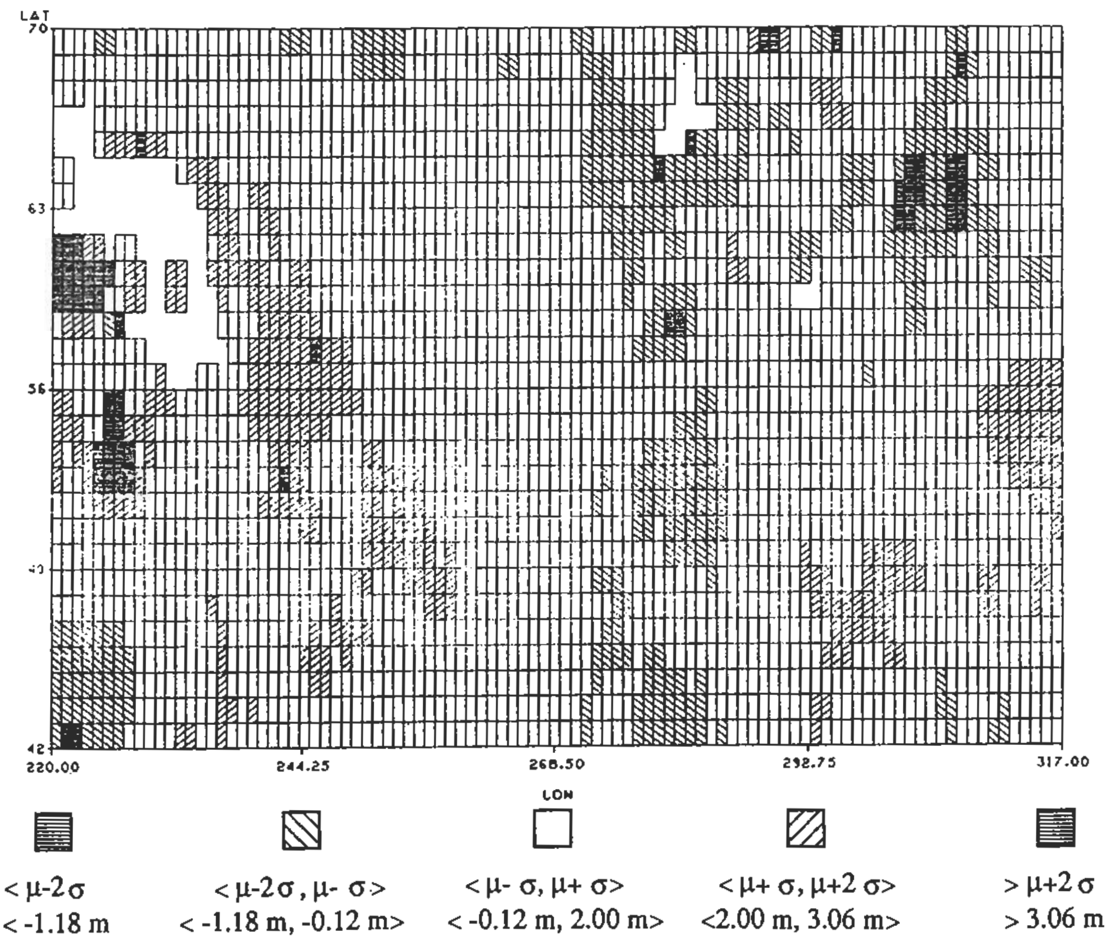

FIGURE 6
Differences [Rapp, 1983b] minus UNB geoid.

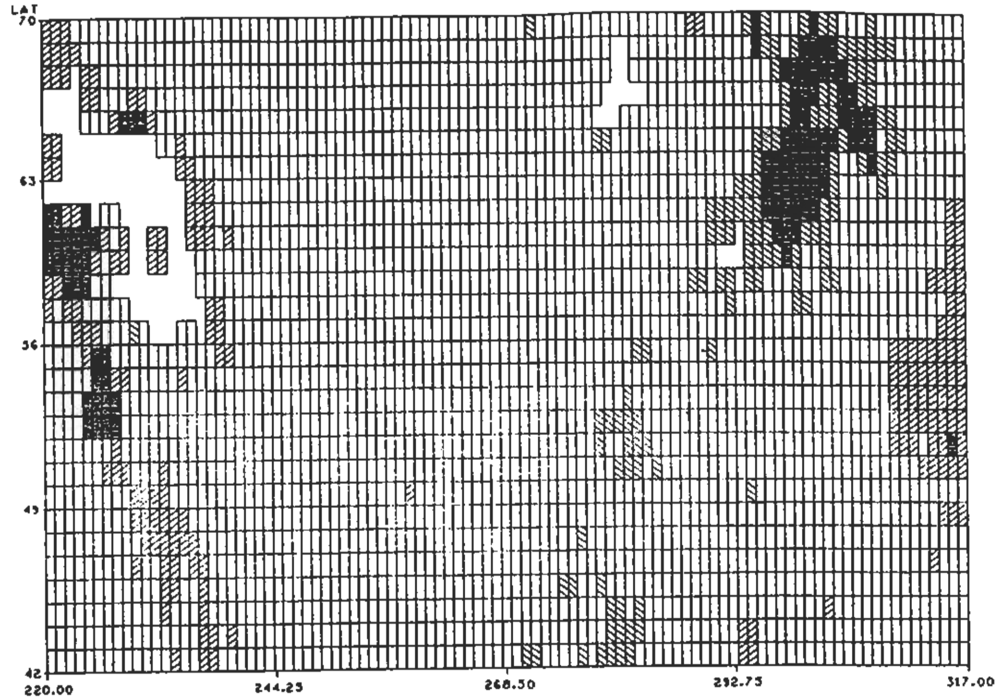

< μ-2σ
< -1.34 m

< μ-2σ , μ- σ >
< -1.34 m, -0.40 m>

< μ- σ, μ+ σ>
< -0.40 m, 1.50 m>

< μ+ σ, μ+2 σ>
<1.50 m, 2.44 m>

> μ+2 σ
> 2.44 m

FIGURE 7
Differences (Wenzel GPM1) minus UNB geoid.

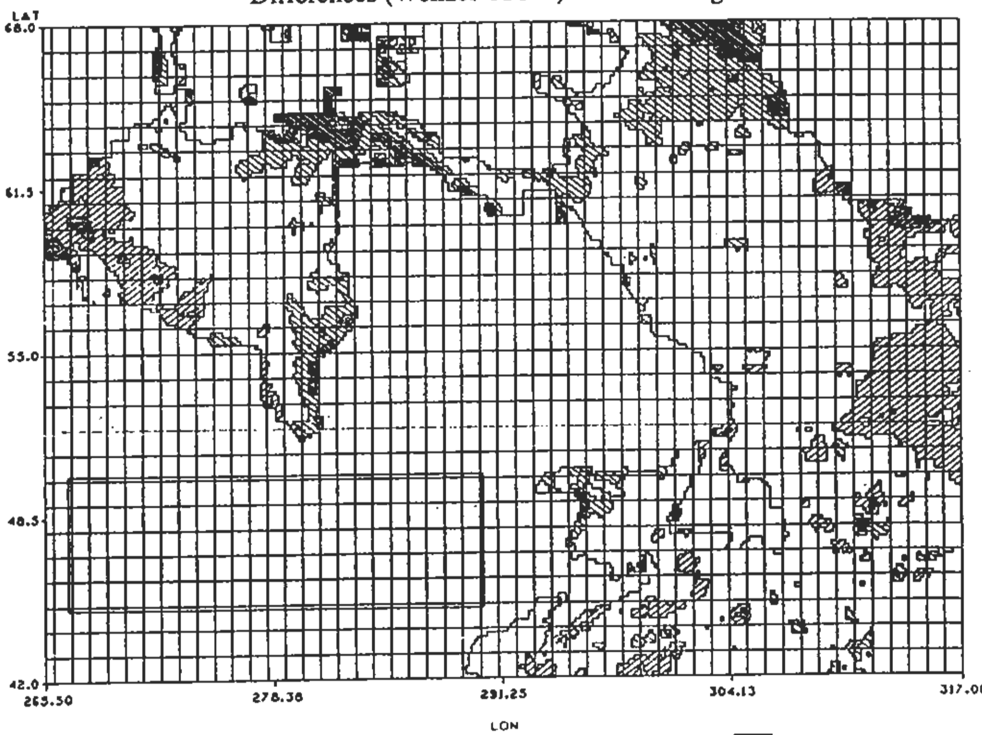

< μ-2σ
< -1.50 m

< μ-2σ , μ- σ >
< -1.50 m, -0.85 m>

< μ- σ, μ+ σ>
< -0.85 m, 0.46 m>

< μ+ σ, μ+2 σ>
<0.46 m, 1.12 m>

> μ+2 σ
> 1.12 m

FIGURE 8
Differences between SEASAT altimetry and UNB gravimetric geoid.

The differences under (a), (b), and (c) reflect the real errors in our as well as the other solutions. Differences from SEASAT altimetry reflect both the real errors and sea surface topography. Some features discernible in Figure 8 are clearly of physical origin and the real error hence is smaller than 65 cm, probably considerably smaller.

All the 'independent' solutions rely, in one way or another, on satellite orbit perturbation analysis. Therefore, the relatively good long wavelength agreement cannot be used as an argument for the long wavelength goodness of our solution. The positive bias of our geoid compared to Wenzel's and to the Doppler points is puzzling. It seems to be either totally absent or at least considerably smaller in the comparison with SEASAT altimetry. Even if one allows for the effect of cooler than average water in the Canadian north and east, the bias in sea surface topography should not reach more than a few decimetres which would not bring the SEASAT and Doppler indicated biases into coincidence.

9. CONCLUSIONS AND ACKNOWLEDGEMENTS

The classical Stokesian solution reformulated for a higher-order reference field combined with the GEM9 (20, 20) reference field have been used to produce a new detailed gravimetric geoid for Canada on a 10' × 10' geographical grid. The solution shows some details hitherto unknown.

The quality of the geoid is difficult to assess objectively because there exists no solution that would be truly independent at least in the long wavelength part of the spectrum. The short wavelength part of our solution looks fairly good — at least from the comparison with SEASAT altimetry — and its accuracy seems to be realistically portrayed by the internal estimates of the standard deviation.

The Stokesian solution, in addition to giving a decent accuracy and to being physically straightforward, is also computationally advantageous. The computation of about 100 000 grid point geoidal heights took about 12 hours CPU time on the UNB IBM 3081 mainframe. The solution on magnetic tape is available upon request from the Geodetic Research Laboratory at UNB.

Other kinds of data, e.g., Doppler points, satellite altimetry, and the deflections of the vertical, should be included in the solution. It is possible to produce corrections to the gravimetric geoid reflecting the other kinds of data, and we are now working on the implementation of one such technique [Vaníček and Kleusberg, 1986].

The work on the new geoid has been carried out at UNB under the terms of a research contract with the Geodetic Survey of Canada and the Natural Sciences and Engineering Research Council of Canada Operating Grant. We wish to acknowledge the contributions to this work made by Messrs. R.-G. Chang, N. Christou, H. Fashir, J. Mantha, M. Hofman, T. Kling and T. Arsenault. Cooperation from the Geodetic Survey of Canada Scientific Authority, Dr. D. Delikaraoglou and the staff of the Division of Gravity, Geothermics and Geodynamics of the Earth Physics Branch of Energy, Mines and Resources Canada has been most appreciated. The comments by two *Manuscripta Geodaetica* reviewers and those received from R.H. Rapp have also been very helpful. The first author was a Swedish Natural Science Research Council Visiting Scholar at the Royal Institute of Technology in Stockholm while preparing the final version of the paper. The SNSRC's support, as well as discussions with Prof. Dr. L.E. Sjöberg, are here gratefully acknowledged. Our thanks go, last but not least, to Ms. W. Wells for her, as usual, flawless wordprocessing as well as language corrections.

10. REFERENCES

Abramowitz, M., Stegun, I.A. (Eds.) (1964). *Handbook of Mathematical Functions*. Dover reprint, 1965.

Ecker, E., Mittermayer, E. (1969). Gravity corrections for the influence of the atmosphere. *Boll. Geoph. Teor. Appl.*, XI, pp. 70-79.

Geodetic Survey of Canada (1985). Personal communication.

Hearty, D.B. (1985; 1986). Personal communication.

Heiskanen, W.A., Moritz, H. (1967). *Physical Geodesy*. Freeman.

International Association of Geodesy (1971). Geodetic Reference System 1967. IAG Special Publication No. 3, Paris, France.

Jekeli, C. (1981). Modifying Stokes' function to reduce the error of geoid undulation computations. *JGR* 84(B8):6985-6990.

Lerch, F.J., Klosko, S.M., Patel, G.B. (1982). A refined gravity model from LAGEOS (GEM-L2). *Geophysical Research Letters*, 9(11):1263-1266.

Lerch, F.J., Klosko, S.M., Laubscher, R.E., Wagner, C.A. (1979). Gravity model improvement using GEOS-3 (GEM9 and 10). *Journal of Geophysical Research*, 84(B8):3897-3916.

Lerch, F.J., Klosko, S.M., Wagner, C.A., Patel, G.B. (1984). Verification of the accuracy of Goddard satellite models. Presented at the AGU Fall Meeting, San Francisco.

Molodenskij, M.S., Eremeev, V.F., Yurkina, M.I. (1960). *Methods for Study of the External Gravitational Field and Figure of the Earth.* English translation by Israel Program for Scientific Translations, Jerusalem, for Office of Technical Services, Department of Commerce, Washington, D.C., 1962.

Moritz, H. (1980). Geodetic Reference System 1980. *Bulletin Géodésique*, 54:395-405.

Paul, M.K. (1973). A method of evaluating the truncation error coefficients for geoidal height. *Bulletin Géodésique*, 57: 413-425.

Rapp, R.H. (1981). Ellipsoidal corrections for geoid undulation computations using gravity anomalies in a cap. *JGR* 86(B11):10843-10848.

Rapp, R.H. (1982). A global atlas of sea surface heights based on the adjusted SEASAT altimeter data. Department of Geodetic Science and Surveying Report No. 333, The Ohio State University, Columbus, Oh.

Rapp, R.H. (1983a). The development of the January 1983 1° x 1° mean free-air anomaly data tape. Internal Report of the Department of Geodetic Science and Surveying, The Ohio State University, Columbus, Oh.

Rapp, R.H. (1983b). The determination of geoid undulations and gravity anomalies from SEASAT altimeter data. *Journal of Geophysical Research*, 88 (C3):1552-1562.

Rapp, R.H. (1986). Personal communication.

Sjöberg, L.E. (1985). A comparison of some modification methods to Stokes' formula using GEM9 potential coefficients. Department of Geodesy Report No. 2, The Royal Institute of Technology, Stockholm.

Vaníček, P., John, S. (1983). Evaluation of geoid solutions for Canada using different data. *Proceedings of the Symposium on Improved Gravity Field Estimation on Global Basis*, Hamburg, August, Vol. 2, pp. 609-624.

Vaníček, P., Kleusberg, A. (1986). Towards a new combined geoid for Canada. To appear in *Proceedings of the International Symposium on the Definition of the Geoid*, Florence, Italy, May.

Vaníček, P., Krakiwsky, E.J. (1982). *Geodesy: The Concepts*. 1st ed., North-Holland, Amsterdam.

Vaníček, P., Kleusberg, A., Chang, R.-G., Fashir, H., Christou, N., Hofman, M., Kling, T., Arsenault, T. (1986a). The Canadian geoid. Department of Surveying Engineering Technical Report, University of New Brunswick, Fredericton.

Vaníček, P., Wells, D.E., Derenyi, E., Kleusberg, A., Yazdani, R., Arsenault, T., Christou, N., Mantha, J., Pagiatakis, S. (1986b). Satellite altimetry applications for marine gravity. Department of Surveying Engineering Technical Report, University of New Brunswick, Fredericton.

Wenzel (1985). Personal communication.

Winter, P.J. (1979). Personal communication.